Senior Honors Thesis
Spring 2010

The Ohio State University
College of Biological Sciences
Department of Biochemistry
Project Adviser: Dr. Donald H. Dean

Characterization of Lysine Mutagenesis in the *Bacillus thuringiensis* Insecticidal Crystal Protein Cry1Ab

Evan Moore

Committee Members:
Dr. Donald H. Dean
Dr. James Hopper
Dr. Michael Ostrowski

Abstract

The insecticidal crystal proteins, known as Cry toxins, are naturally derived from *Bacillus thuringiensis* and provide an environmentally safe form of pest control. Though these proteins have been studied extensively, little is known regarding their specific mechanism of action and any conformational changes associated with this mechanism. In an effort to design a mutant Cry1Ab toxin with two individual lysine and cysteine residues for fluorophore ligation, this study focuses on the characterization of the structural effects of lysine mutagenesis leading to future development of such a toxin. In this study, the three lysines of active Cry1Ab toxin are mutated to alanine in different combinations, and the structural effects of these mutations are monitored by SDS-PAGE, bioassay, and circular dichroism wavelength scanning. Structural analyses have revealed that mutation of lysine 490 to alanine results in a toxin with increased protease sensitivity that makes isolation of pure, active toxin by the standardized procedure extremely difficult. Mutations of the other lysine residues are shown to have a lesser effect on toxin structure. The observations of this study contribute to data regarding potential sites on Cry1Ab for ligation of functional groups, and the structural and functional effects of mutagenesis at these sites.

Acknowledgements

I would like to express my utmost appreciation to Dr. Dean for his immense impact in shaping my undergraduate education and for his continued guidance and support as I develop laboratory skills and acumen.

I would also like to thank the members of the Dean lab for their guidance and support, particularly Dr. Manoj Nair who has been instrumental in my development as a young researcher.

Finally I would like to thank the members of my defense committee for their sacrifice of valuable time and their criticisms, which I look forward to hearing.

Thank you all,

Evan Moore

Introduction

The insecticidal crystal proteins, known as Cry toxins, produced by sporulating *Bacillus thuringiensis* (Bt) have been a subject of intensive research for their potential in agricultural applications as biologically derived and biodegradable pesticides. In a time when environmental issues, such as the environmentally damaging use of chemical pesticides, are receiving much attention, a naturally derived pesticide with minimal ecological implications provides a more responsible form of pest control. Each toxin within this large family of proteins is typically specific to only one or a few species within an order, depending, at least in part, on the aminopeptidase N (APN) and cadherin-like receptor types found in the midgut epithelial cells of the target organism (1). Typically, the toxin is ingested by a susceptible insect as an insoluble inclusion body and is solubilized by the alkaline conditions within the insect's midgut, where proteolytic processing cleaves portions of the carboxy terminus and sometimes also the amino terminus (2). In the case of Cry1Ab, this means the processing of a 130 kDa protoxin to a 65 kDa active toxin through extensive trypsinization of the carboxy terminus and more minor processing of the amino terminus. Solubilization and proteolytic processing then leads to receptor binding at APN and/or cadherin-like receptors and insertion of the toxin into epithelial cell membranes forming ion channels or pores leading to insect death. Crystallographic data of the closely related Cry1Aa protein (3) suggests that Cry1Ab has a three domain structure. Domain I consists of seven α-helices forming a bundle around α-helix 5, and α-helix 1 is believed to be cleaved at some point after or prior to membrane insertion (4). Evidence supports that domain I functions primarily in membrane insertion and pore formation (5). Domain II takes on a β-prism fold of three β sheets arranged in a

Greek key motif and its loop regions have been shown to affect receptor binding (6,7). Domain III forms a β-sandwich "jelly roll" topology of two twisted, antiparallel β-sheets and is also related to receptor binding (8,9). *Figure 1* shows Cry1Ab with its three domains and three lysines color coded (based on PDB file 1CIY for Cry1Aa). The mechanism and extent of toxin insertion has been a subject of some dispute. Current models, such as the "umbrella model" and the "penknife model," suggest that α-helices 4 and 5 (the umbrella model) or 5 and 6 (the penknife model) of domain I penetrate the epithelial cell membrane to form an ion pore in response to receptor binding, leaving the remainder of the toxin outside the membrane (10). Evidence has been found, however, that portions of both domains II and III can insert into brush border membrane vesicles, suggesting that the extent of membrane insertion may be greater than the above mechanisms would allow (11). In summary, though the structure and activities of Cry1Ab have been well characterized, the true molecular dynamics of receptor binding, membrane insertion, and pore formation have yet to be well characterized.

In an effort to shed light on the conformational dynamics of Cry1Ab, this project began with the goal of analyzing intramolecular Förster resonance energy transfer (FRET) between fluorophores attached to cysteine and lysine residues of the active toxin. As the wild type, active toxin contains three lysine residues and no cysteine residues, one cysteine would have to be introduced and two lysines removed to provide two distinct moieties for fluorophore ligation. In the event that structural and functional analyses of such a mutant toxin would show it to be insignificantly perturbed by such mutagenesis and labeling, changes in FRET response could quantitatively describe distances between structural elements in solution and in response to receptor binding and membrane

insertion. After site-directed mutagenesis by PCR with mutagenic primers, purification of a mutant toxin revealed the significance of at least one lysine residue on structural stability or expression. The significance of lysine residues on the structure and stability of Cry1Ab, by necessity, had to be addressed and is the focus of this work. Successive mutagenesis of lysine to alanine at residues 403, 478, and 490 provided three single mutants, two double mutants (K478A/K490A further referred to as DM1 and K478A/K403A further referred to as DM2), and one triple mutant (TM). These are the six mutant strains characterized in this study. After isolation of each pure toxin variant, structure, stability, and functionality were addressed by SDS-PAGE, bioassay, and wavelength scanning circular dichroism. The true value of this study lies in the characterization of lysine mutagenesis for the sake of using lysine residues as sites for the binding of markers, fluorophores, or other functional groups.

Materials and Methods

Site-directed Mutagenesis, Transformation, and Confirmation of Expression

The cry1Ab9-033 gene (12), originally provided by Dr. T. Yamamoto (Sandoz Agro Inc., Palo Alto, Calif), was previously inserted into Stratagene's PBluescript vector, and was kindly provided as such by Dr. Manoj S. Nair (Biochemistry Department, The Ohio State University). Mutagenesis was carried out by PCR using EMD Biosciences' KOD Hot Start DNA Polymerase and its corresponding reaction components to a 50 µl reaction volume. Mutagenic primers were ordered online from Sigma Aldrich. Parental DNA was DpnI (1 µl, 20,000 U/ml, New England BioLabs) digested for 1 hour before transformation to chemically competent DH5α, prepared by $CaCl_2$ treatment (OD_{600} of

0.4-0.5). Plasmid DNA was purified for sequencing using the QIAGEN QIAprep® Spin MiniPrep Kit as described in the manufacturer's manual. Positive mutagenesis was confirmed by plasmid sequencing at The Ohio State University's Columbus campus Plant Microbe Genomics Facility. Toxin expression was confirmed by 8% polyacrylamide SDS-PAGE analysis of cellular or protein extracts.

Large Scale Expression and Purification of Toxin Mutants

Expression and purification methods were performed based on the procedure detailed by Lee et al (7). Cell cultures were grown for 72 hours at room temperature in sterile, modified "Terrific Broth" media (0.034 M KH_2PO_4, 0.144 M K_2HPO_4, 10 ml glycerol / 500 ml broth) with 0.1 mg/ml ampicillin. Cells were pelleted by centrifugation for 10 minutes at 8,000 rpm, resuspended in 100 ml sterile lysis buffer (50 mM Tris, 50 mM EDTA, 15% sucrose, pH 8.0) to which 0.12 g lysozyme was added, and incubated with shaking at 37°C overnight. The lysis suspension was then centrifuged as above, the pellet was resuspended in 100 ml "Crystal Wash I" (0.5 M NaCl, 2% Triton X-100), and the resuspension was sonicated on ice for two, five minute (10 seconds on, 10 seconds off) sessions separated by 2 minutes for cooling. This sonicate was then centrifuged as above and "washed" by resuspension and centrifugation three times with Crystal Wash I, followed by three washes with "Crystal Wash II" (0.5 M NaCl). The resulting washed pellet was resuspended and solubilized for 3 hours with mixing at 37°C in 50 mM Na_2CO_3 buffer, pH 10.5, with 2% 2-mercapto ethanol followed by trypsin digestion (2% wt/wt) under the same conditions for 30 minutes. Solubilized, trypsined toxin was then purified by Q Sepharose™ High Performance ion exchange resin (5 ml, GE Healthcare)

and eluted from this resin with 30-50 ml 0.15 M NaCl, 50 mM Na_2CO_3 buffer, pH 10.5. Both flow through and elution fractions were then loaded to a 300 ml column of Sephacryl® S-300 HR resin and eluted with 0.5 M NaCl, 50 mM Na_2CO_3 buffer, pH 10.5, over 20 ~17.5 ml fractions. The fractions containing active toxin, as identified by SDS-PAGE (a pair of bands around 65 kDa), were concentrated by centrifugation at 3,500 rpm in Amicon® Ultra centrifugal filter devices with molecular weight cut off of 50 kDa (Millipore). Phenylmethanesulfonylfluoride (PMSF) was added to 1 mM concentration to samples after activation by trypsinization to prevent excessive degradation. Sodium azide was added to "crystal washed" pellets that were to be stored overnight or longer to prevent bacterial growth. Purified toxin samples were stored at 4°C.

Mutant Toxicity Bioassays

Mutant toxicity bioassays involved the analysis of percent mortality of *Manduca sexta* larvae across a concentration range. Two types of bioassay were performed, diet incorporation (WT and K490A) and surface treatment (WT, K478A, K403A, DM2), for reasons detailed in the results section. 1 ml tobacco hornworm growth media (www.bio-serv.com), treated with the anti-fungal agent aureomycin, was aliquoted to each well of one 24-well polystyrene plate (2 cm^2 wells, Falcon) per mutant strain. For the two, diet incorporation assay plates, 90.2-190.8 ul "Crystal Washed" insoluble protein suspension was incorporated into the hardening diet (50% normal agar added) across the concentrations 0, 15, 30, 60, 90, 120, and "lethal" (undiluted) ng/ml. For the four, surface treatment assay plates, 50 ul purified toxin dilution was added to the center of the hardened growth media across the concentrations 0, 1, 5, 10, 20, 30, and 50 ng/cm^2. After

media and toxin were hardened and dry, two *Manduca sexta* larvae (neonate or 1st instar developmental stage, hatched from eggs purchased from Carolina Biological Supply Company) were added to each well such that four larvae were tested in both the highest and lowest (control) concentrations, and eight larvae were tested in all other concentrations. The number of living and dead larvae was recorded after 5, 8, and 11 days. Pictures of the bioassay plates were taken after 11 days, prior to freezing at -20°C for disposal.

Toxin Secondary Structural Analysis by Wavelength Scanning Circular Dichroism

Toxin secondary structure was analyzed by wavelength scanning circular dichroism using an Aviv Circular Dichroism Spectrometer (Model 62A DS) for WT, K478A, K490A, K403A, and DM2. Toxin samples stored in 0.5 M NaCl 50 mM Na_2CO_3 buffer, pH 10.5, were loaded to PD-10 Desalting Columns (GE Healthcare) and eluted with 50 mM Na_2CO_3 buffer, pH 10.5. Ten scans were averaged across the 195-300 nm wavelength range sampling every 1.0 nm, with 300 ul sample volumes at a concentration of 2 μM.

Results

Expression and Purification of Toxin Mutants

Successful transformation of mutagenized Cry1Ab genes to chemically competent DH5α cells via the PBluescript vector was confirmed by plasmid preparation and sequencing at the Plant Microbe Genomics Facility (The Ohio State University, Columbus Campus). Expression of the mutant toxin was confirmed by the presence of a 130 kDa band on an 8% SDS-polyacrylamide gel that was replaced by a pair of bands

(likely the result of multiple trypsin sites at the C-terminus of the activated toxin) at 65 kDa after activation by trypsin digestion. An early mutant strain, dubbed S41C, containing the mutations K478A, K490A, and S41C was found to be sensitive to the purification procedure, disappearing entirely after trypsinization as shown in *Figure 2* (The molecular weight marker shown in this figure is the same throughout all SDS-PAGE gels). Suspecting lysine mutagenesis to be the factor leading to this trait, the mutant toxins K478A, DM1 (K478A, K490A), TM (K478A, K490A, and K403A), and the WT toxin were solubilized for 3 hours, trypsinizing a sample of each for 30 minutes after each hour. *Figure 3* shows that regardless of the time spent solubilizing the toxin, it is the addition of the K490A mutation that results in the loss of toxin. Bradford assays run during this procedure indicated a ~2.7 fold decrease in total protein from the wild type to the single mutant K478A, and a ~1.8 fold decrease in total protein from the single mutant K478A to the double mutant DM1, but no significant change in concentration between the double and triple mutant.

After identifying the problematic mutation, single and double mutants (K478A, K490A, K403A, DM1 (K478A, K490A), and DM2 (K478A, K403A) were grown to more fully characterize the observations from previous mutants. *Figure 4* shows the effects of the K490A mutation, both as a single mutant and in DM1.

Mutant Toxicity Bioassays

Mutant toxicity, interpreted as percent mortality, was recorded after 5, 8, and 11 days taking pictures of the bioassay plates on the 11^{th} day. WT and K490A toxins were compared by diet incorporation of the “crystal washed” pellet protein extract, as the intact form of K490A was difficult to obtain, but should still be toxic when ingested in this

form. WT, K478A, K403A, and DM2 were compared by surface treatment. Diet incorporation assays were generally unsuccessful in establishing the typical proportionality between increasing concentration and percent mortality, probably because actual toxin concentrations are difficult to estimate in the mixture of protein crystals added. The most interesting data obtained from these plates was with respect to the four larvae treated at very high (undiluted) crystal concentrations, of which 75% died for the WT toxin and 100% died for K490A, suggesting the K490A is still toxic.

The clearest data were achieved after 5 days and are described in *Figure 5*. These data show a general increase in percent mortality with an increase in the surface concentration of the toxin, particularly for the WT and K478A toxins. K403A and DM2 toxins showed no significant trend in percent mortality with respect to surface concentration, which could be an indication of disrupted function or complications in assay preparation. Significant, however, is the appearance of the larvae after 11 days. Regardless of survival rate, a noticeable inverse relationship between toxin concentration and larval development can be observed in *Figure 6*, suggesting that the larvae had ingested enough toxin to cripple their metabolic functions, at which point their eating behavior ceased and they began to slowly starve to death. This could indicate that all toxin variants still maintain some degree of toxicity.

Toxin Secondary Structural Analysis by Wavelength Scanning Circular Dichroism

Secondary structural analysis by wavelength scanning circular dichroism was performed for WT, K478A, K403A, and DM2 toxins at 2 μM and K490A at 1.8 μM. Problematic toxin preparation of K490A, as described above, has prevented analysis of K490A at 2 μM up to this point. These data are shown in *Figure 7*, which shows the most

significant structural perturbations for K490A and DM2 where K478A and K403A show curves that describe structural elements similar to that of the WT toxin. K490A's spectrum shows a decrease in overall alpha helical character, and DM2's spectrum may suggest a decrease in alpha helical tertiary interactions. As significant amounts of active DM1 could not be purified and isolated, this mutant was not analyzed by wavelength scanning circular dichroism.

Discussion

From the results observed during protein purification of S41C, K490A, and DM1 (*Figures 2-4*), the mutation of lysine 490 to an alanine disrupts the stability and total yield of the activated toxin. Considering that the DNA and expression vector, as well as the promoter from which the modified Cry1Ab gene was expressed, was the same as the WT for each mutant, it is unlikely that the mRNA expression of the gene has been reduced. It has been previously noted that certain mutations can lead to mutant protoxins and/or toxins that cannot be isolated, potentially due to an increase in protease sensitivity or access to protease sites as a result of alterations in the protein stability or structure (13). This observation correlates well with the data in *Figure 7*, showing K490A, which had the lowest yield, to be the most destabilized structure.

Looking at the SDS-PAGE gels shown in *Figures 2-4*, it is apparent that the mutation K490A has a significant effect on the stability of the toxin. Frames A and B of *Figure 2* show that S41C protoxin could be solubilized, but after trypsinization (lane 2, frame B), the active toxin band (65 kDa) is not seen. Instead, a pair of dark bands, that can also be observed in the WT prep in *Figure 2* Frame D, appear below the 37 kDa marker. These bands may represent degraded fragments of the active toxin. Though one

may not expect removal of a lysine (potential trypsin cleavage site) to increase the extent of cleavage, my supposition is that alteration of the toxin's structure, due to destabilizing effects as a result of the K490A mutation, may expose other trypsin sites or sites sensitive to cleavage by other proteases. *Figure 3* shows that regardless of the time spent solubilizing the protein pellet, addition of the K490A mutation has, at lease visibly, prevented isolation of even the protoxin. Though yield was decreased by addition of each successive mutation (except for the 3rd and final mutation, K403A), it is noted that the visible presence of bands running at molecular weight 50 kDa and smaller suggests that these are the principle species, and the visible absence of protoxin and toxin bands is not due to an overall lack of protein. Though protein concentration from left to right across these gels decreases, these bands remain present, indicating that their relative amount is increasing with respect to protoxin and toxin. It must also be noted that particularly for TM, and a lesser extent for DM1, the same pair of bands below the 37 kDa marker can be seen as was observed in *Figure 2*. These $\leq$ 50 kDa bands appear to be present, at least to some degree, in all lanes of *Figure 3*, Frame B, suggesting that these bands are possible degradation products of Cry1Ab.

These observations are reiterated in *Figure 4*, which represents separate preparations of the K490A and DM1 mutant toxins. Frame A shows a band just below the 75 kDa marker in lanes 2 and 3 that is likely an already partially degraded form of the protoxin, that is partially converted to the active form after trypsinization (lane 3). Odd, however, is the almost complete absence of protein in lanes 4 and 5 (after ion exchange column purification). Frame B shows the end result of this K490A prep from which a small amount of K490A was successfully purified, but in the presence of the degraded

bands ≤ 50 kDa. Frame C representing the purification of DM1 first shows in lane 1 the purified form of DM2 active toxin as a reference for a stably prepared double lysine mutant. The remaining lanes show the purification of DM1 in which the above observations can be seen again as the protein concentration density shifts away from larger species like the protoxin and toxin toward the degraded bands around or below 50 kDa. As the difficulty experienced in purifying K490A containing mutants seems to be related to protease sensitivity, any future attempts at purification of such mutants should analyze the effect of shorter trypsin digestions and more delicate storage and handling techniques.

Bioassay experiments performed in this study showed a clear proportionality between percent mortality and toxin surface concentration 5 days after treatment, as shown in *Figure 5*, and as previously observed (11). Though percent mortality calculations for the diet incorporation assays were not useful for analysis, the observation that the undiluted crystals were still lethal lends credence to the likelihood of K490A's toxicity. The photographs of the six bioassay plates shown in *Figure 6* show a clear inhibition of larval growth and development as toxin concentrations increase from left to right (highest and lowest (0) concentrations, however, are the first column of four wells, highest being the top two and lowest being the bottom two), as has previously been observed for Cry1Ab (14). These plates support the conclusion that the toxins studied may have lost some degree of toxicity relative to the WT, but are still functional.

Wavelength scanning circular dichroism is a tool that is commonly used to analyze protein secondary and/or tertiary structures (http://www.ap-lab.com/circular_dichroism.htm). The dominant form of secondary structure in Cry1Ab is

the alpha helix (as can been seen in *Figure 1*, Frame A), and the observed elipticity response spectra shown in *Figure 7* generally agree with a predominantly alpha helical structure. The patterns observed in *Figure 7* for WT with respect to the mutants K478A and K403A shows only minor deviations in secondary structure, indicating that these mutants have a secondary structure similar to that of the WT toxin. K490A's CD spectrum shows an upward shift in elipticity, and a softening of the two alpha helical minima typically found at 220 and 208 nm (15). This could be an indication of a loss of secondary structural elements in conjunction with a spectral shift toward a structure with more random coil nature, but could also be related to the lower concentration analyzed by necessity, as described earlier. If K490A's CD spectrum is, in fact, an indication of an increase in random secondary structure, it could explain the apparent increase in protease sensitivity for this mutant. DM2's CD spectrum shows a shift in the opposite direction, particularly around wavelength 208 nm, which may be an indication that the mutations of DM2 have led to a decrease in tertiary interactions of alpha helices (16).

Thermal denaturation of Cry1Ab toxins can be observed by circular dichroism signal at 223 nm and reflects the thermal stability of the protein (17). Preliminary work in an effort to achieve this data has been done (*Figure 8* Frame A), but an SDS-PAGE gel (*Figure 8* Frame B) has shown the WT toxin used for this data was degraded. Significant levels of impurities preclude this data from speculation until reliable WT data can be achieved.

Figure 9 shows the successfully purified forms of each toxin analyzed in this study. Following the same procedure in each preparation, K490A and DM1 mutants could not be purified as was the case with other single or double mutants. Based on the

combined results of SDS-PAGE analysis, bioassay, and circular dichroism wavelength scanning, I would conclude that the K490A mutation, whether alone or in combination with the K478A mutation, yields a toxin with a secondary structure similar to that of the WT, but perhaps loose enough in conformational flexibility that cellular proteases, as well as the protease treatment procedurally applied in toxin activation, digest the protein to fragments $\leq$ 50 kDa before useable quantities can be isolated.

Looking back at the work described in this study, it has become clear to me that lysine 490 should not be mutated to alanine. This, however, does not mean that it cannot be used for fluorophore ligation. The next step in my research will be an analysis of the accessibility and binding of fluorescent tags to unmutated Cry1Ab toxin. It is my prediction that lysine 478 may not be accessible to amine reactive ligation, where lysines 490 and 403 will likely be accessible. If this is the case, lysine 478 may not need to be removed, reducing the structural stress of creating double mutants. As lysine 490 should be left unmutated, a K403A mutant could then provide a single, accessible lysine for fluorophore ligation. If this succeeds, and the structure of the fluorophore ligated toxin can be shown to be close to the WT structure, cysteine mutants could be developed by a similar process to provide the other fluorophore ligation site necessary for FRET analysis.

Figures

Figure 1: Location of lysine residues within Cry1Ab structure (based on PDB file 1CIY for Cry1Aa)

A B

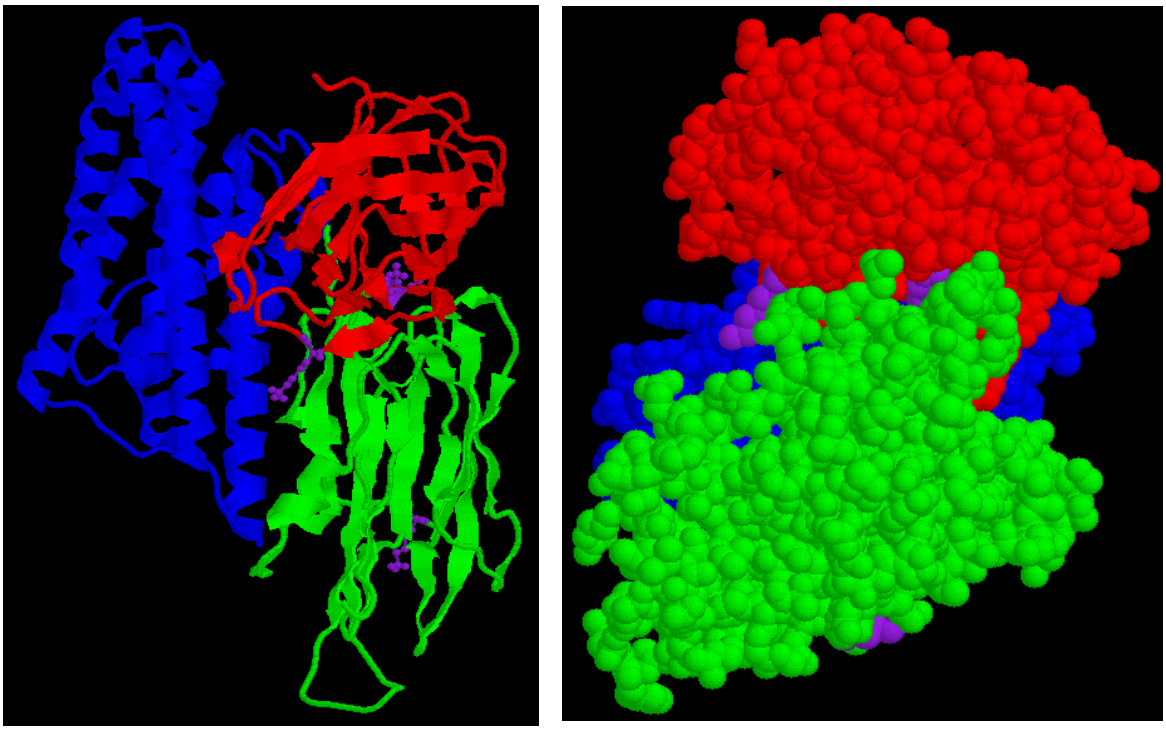

Frame A: Cartoon model showing positions of lysine 403 (bottom), 478 (top), and 490 (left) with domain I in blue, domain II in green, and domain III in red

Frame B: Spacefilling model with the same color coding to illustrate the relative depths of the three lysines with 478 buried, 490 exposed in a pocket, and 403 surface level

Figure 2: S41C Purification Analysis

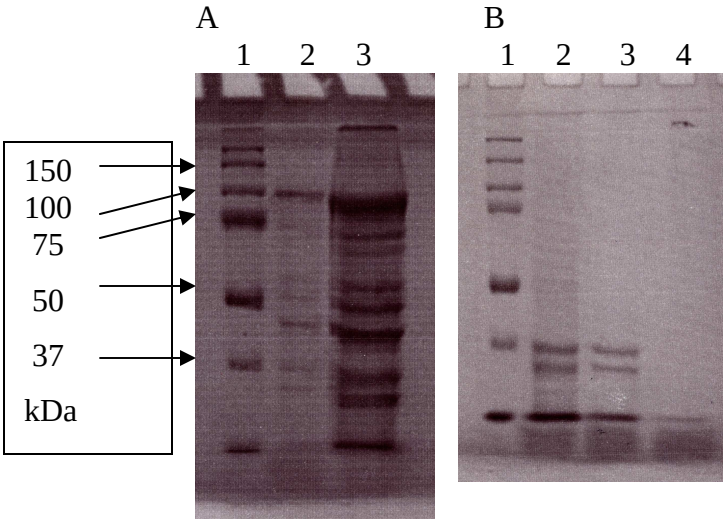

Frame A: Lane (1) MW marker (2) 1/10 dilution solubilized S41C (3) solubilized S41C
Frame B: Lane (1) MW marker (2) trypsinized S41C (3) S41C ion exchange column flow through (4) S41C ion exchange column elution

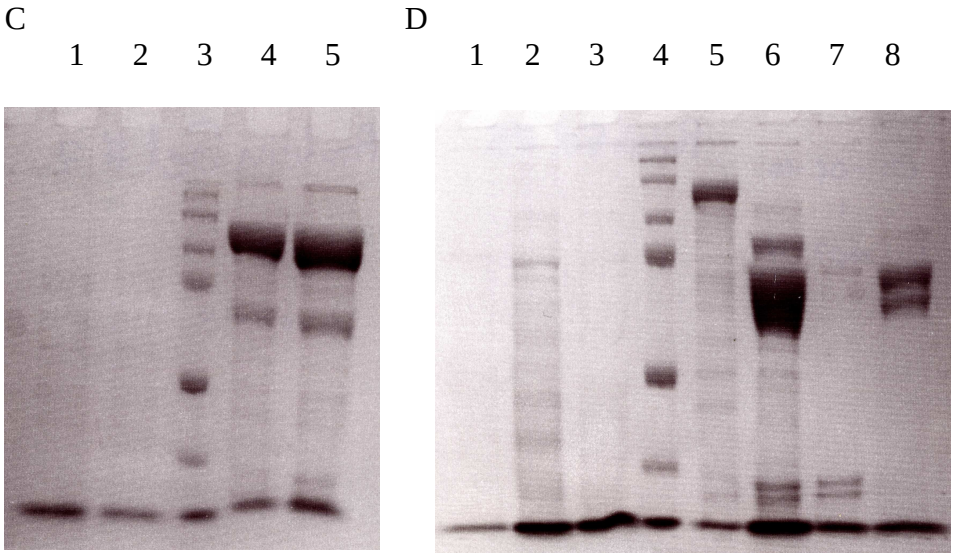

Frame C: Lane (1) solubilized S41C (2) ½ dilution solubilized S41C (3) MW marker (4) ½ dilution solubilized WT (5) solubilized WT
Frame D: Lane (1) 1/10 dilution solubilized S41C (2) solubilized S41C (3) trypsinized S41C (4) MW marker (5) 1/10 dilution solubilied WT (6) trypsinized WT (7) WT ion exchange column flow through (8) WT ion exchange column eluant

Figure 3: Solubilization and trypsinization of successive lysine deletions over time

Frame A: Lane (1) MW marker (2,3) WT solubilization/trypsinization (4,5) K478A solubilization/trypsinization (6,7) DM1 solubilization/trypsinization (8,9) TM solubilization trypsinization all after 1 hour solubilization

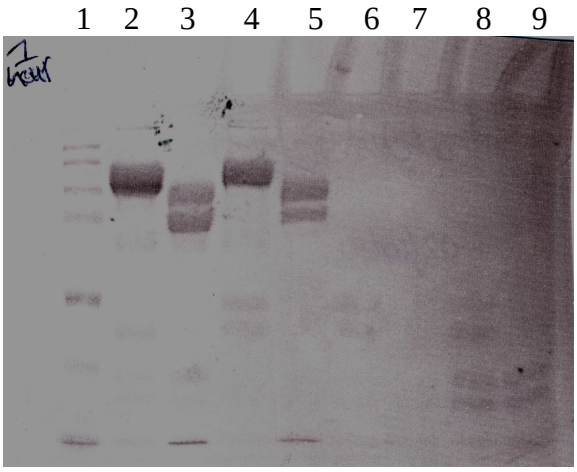

Frame B: Lane (1) MW marker (2,3) WT solubilization/trypsinization (4,5) K478A solubilization/trypsinization (6,7) DM1 solubilization/trypsinization (8,9) TM solubilization trypsinization all after 2 hour solubilization

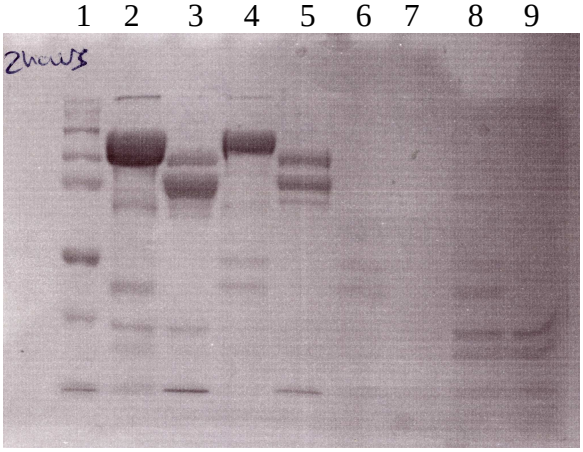

Frame C: Lane (1) MW marker (2,3) WT solubilization/trypsinization (4,5) K478A solubilization/trypsinization (6,7) DM1 solubilization/trypsinization (8,9) TM solubilization trypsinization all after 3 hour solubilization

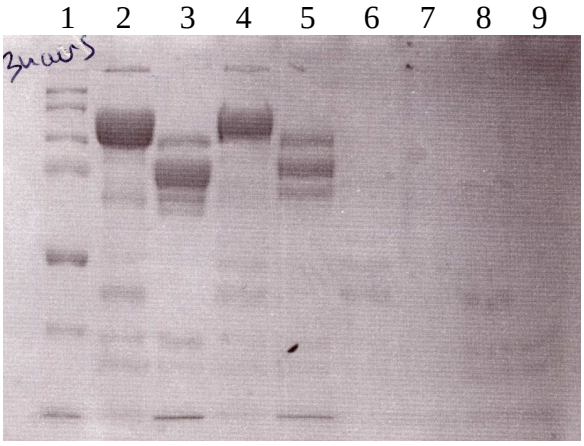

Figure 4: Purification of K490A and DM1

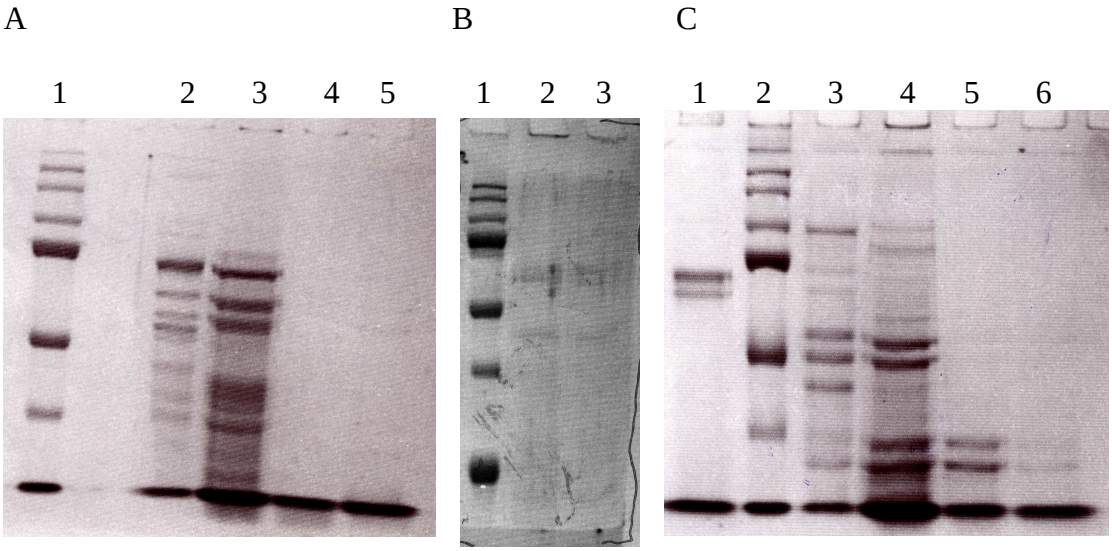

Frame A: Lane (1) MW marker (2) 1/10 dilution K490A solubilization (3) K490A trypsinization (4) ion exchange column flow through (5) ion exchange column eluant

Frame B: Lane (1) MW marker (2) purified K490A in 0.0 M NaCl 50 mM Na_2CO_3 buffer, pH 10.5 (3) purified K490A in 0.5 M NaCl 50 mM Na_2CO_3 buffer, pH 10.5

Frame C: Lane (1) purified DM2 in 0.0 M NaCl 50 mM Na_2CO_3 buffer, pH 10.5 (2) MW marker (3) 1/10 dilution DM1 solubilization (4) DM1 trypsinization (5) ion exchange column flow through (6) ion exchange column eluant

Figure 5: Surface treatment bioassay mortality 5 days after treatment

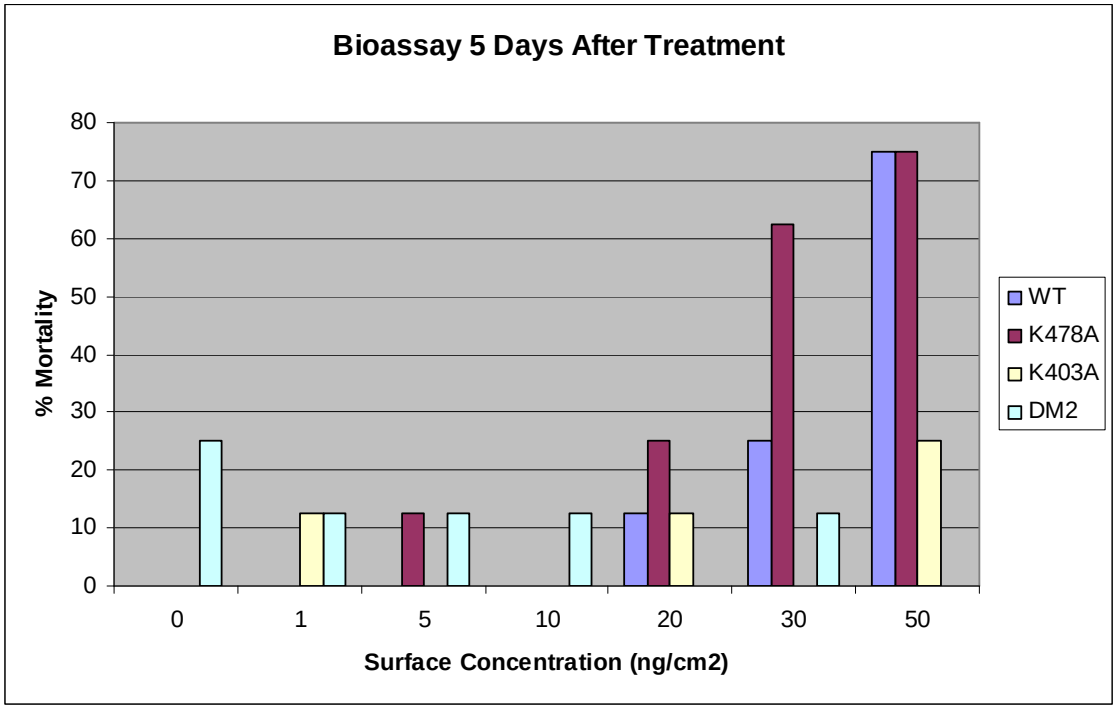

Figure 6: Photographs of bioassay plates 11 days after treatment

Diet Incorporation Bioassays

WT

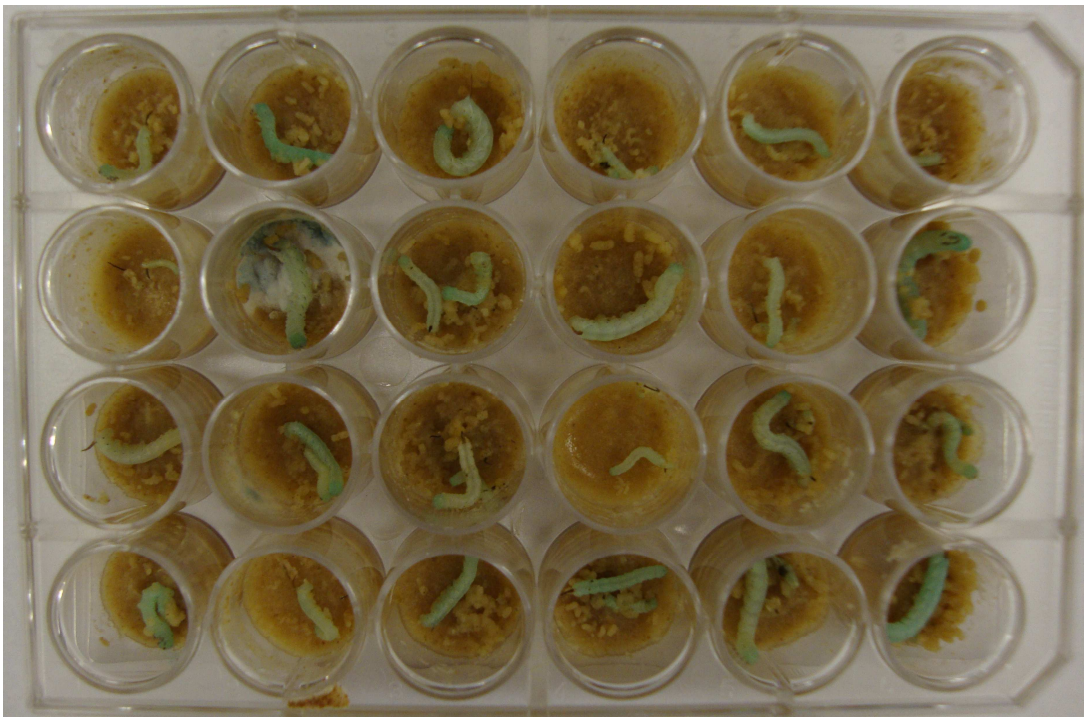

K490A

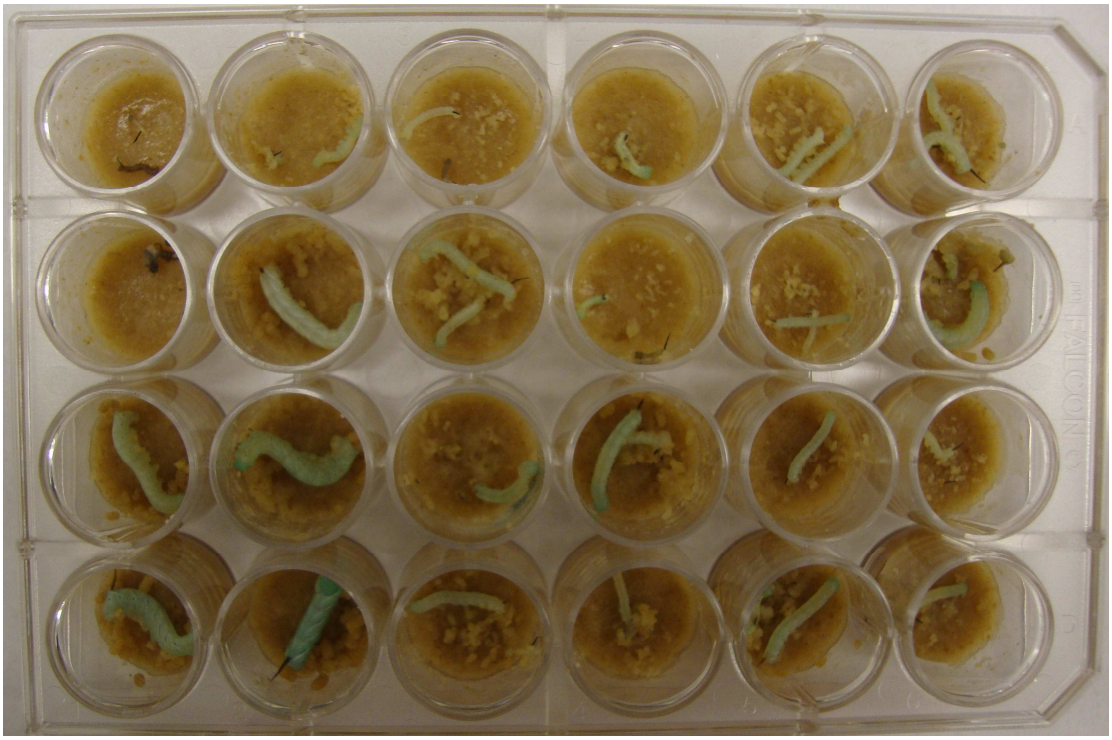

Surface Treated Bioassays

WT

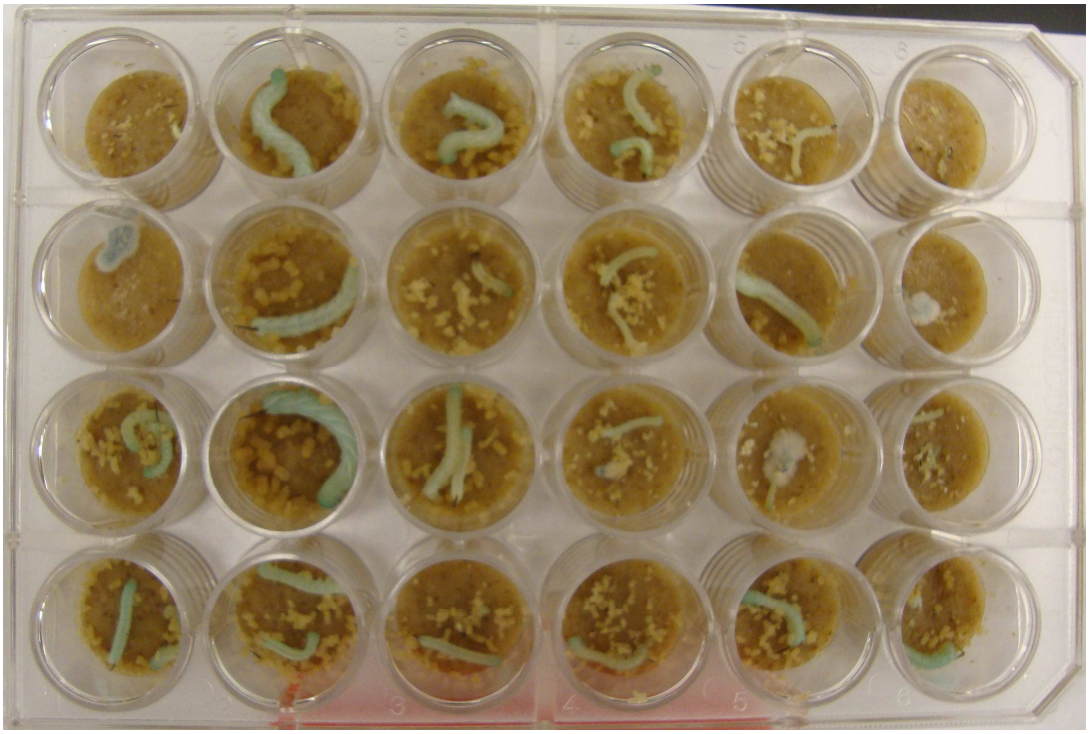

K478A

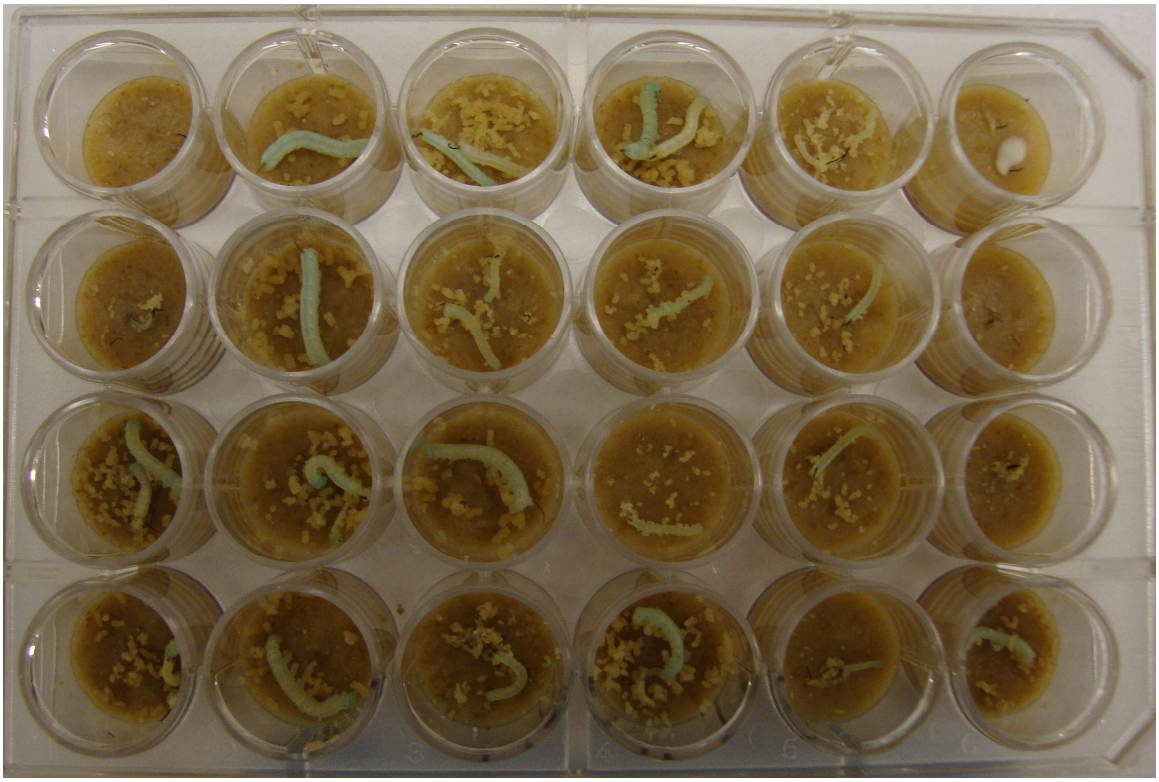

K403A

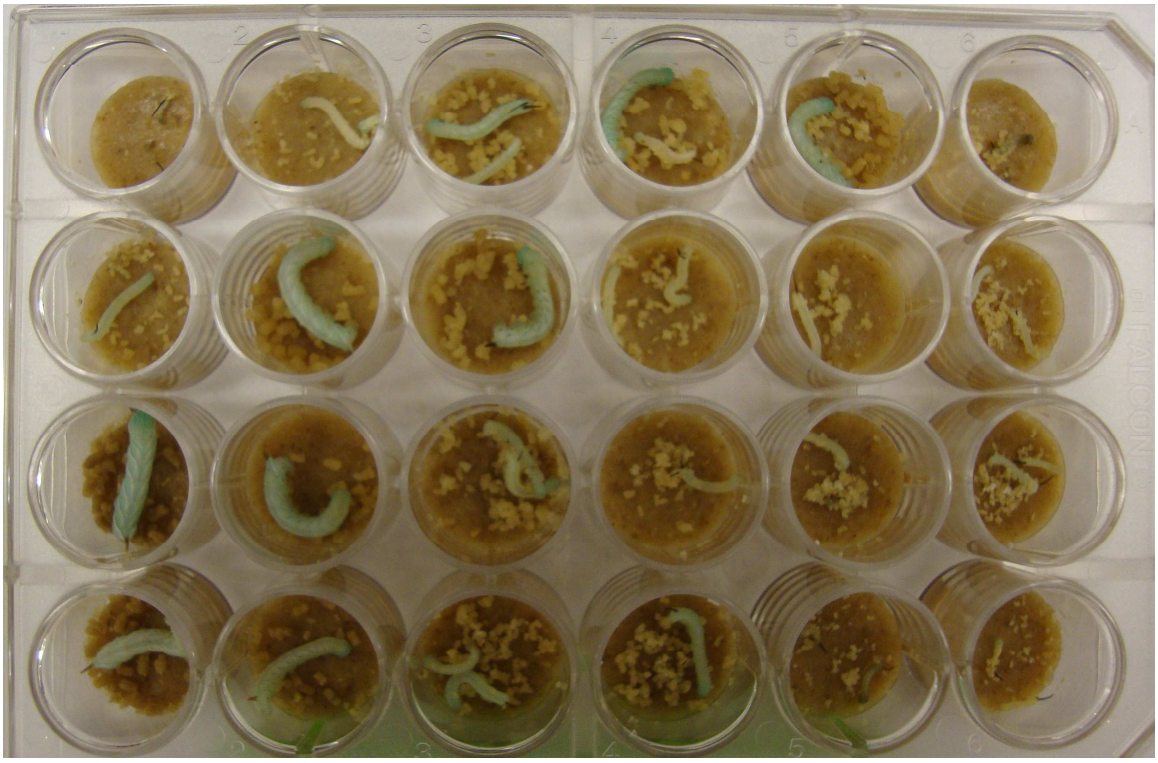

DM2

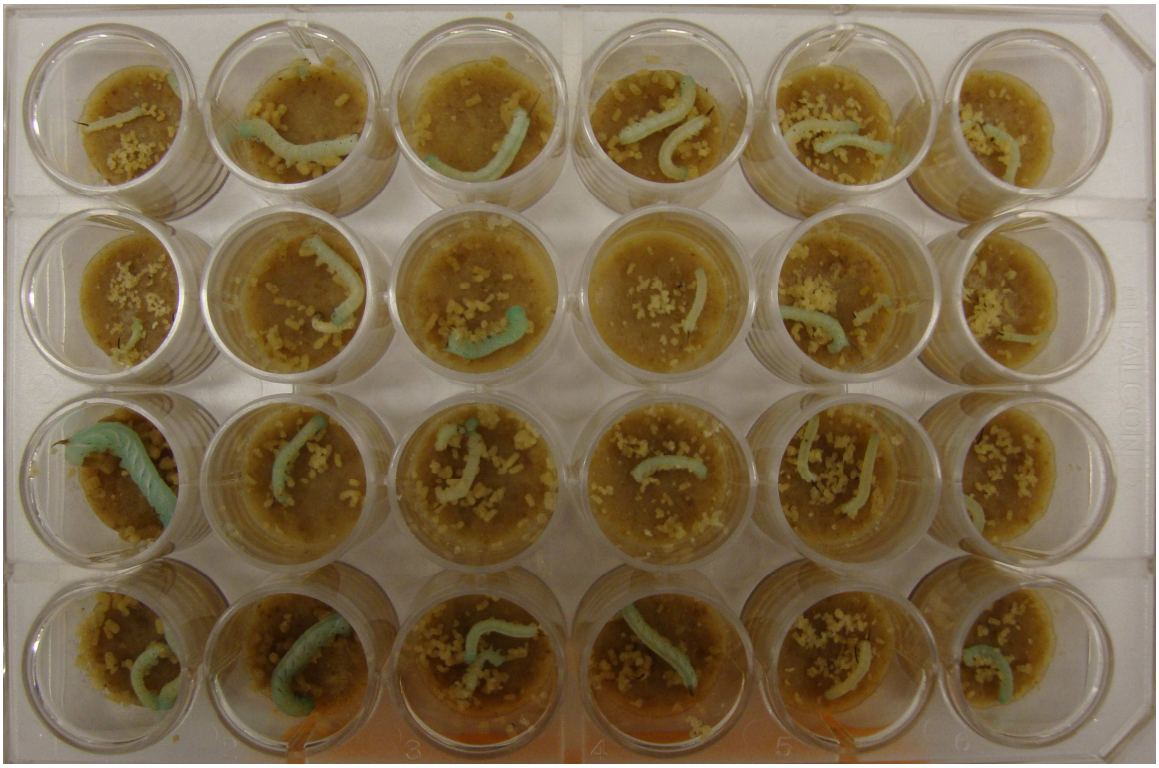

Figure 7: Mutant toxin wavelength scanning circular dichroism spectra

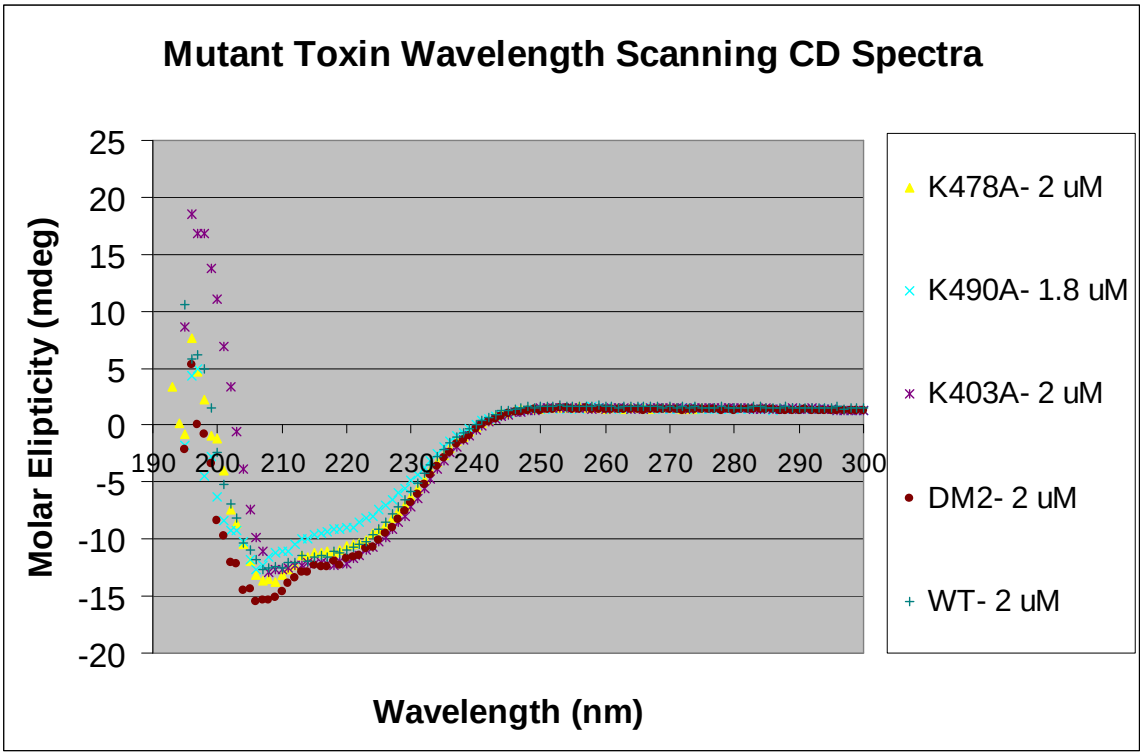

Figure 8: Mutant toxin thermal denaturation analyzed by circular dichroism at 223 nm

Frame A

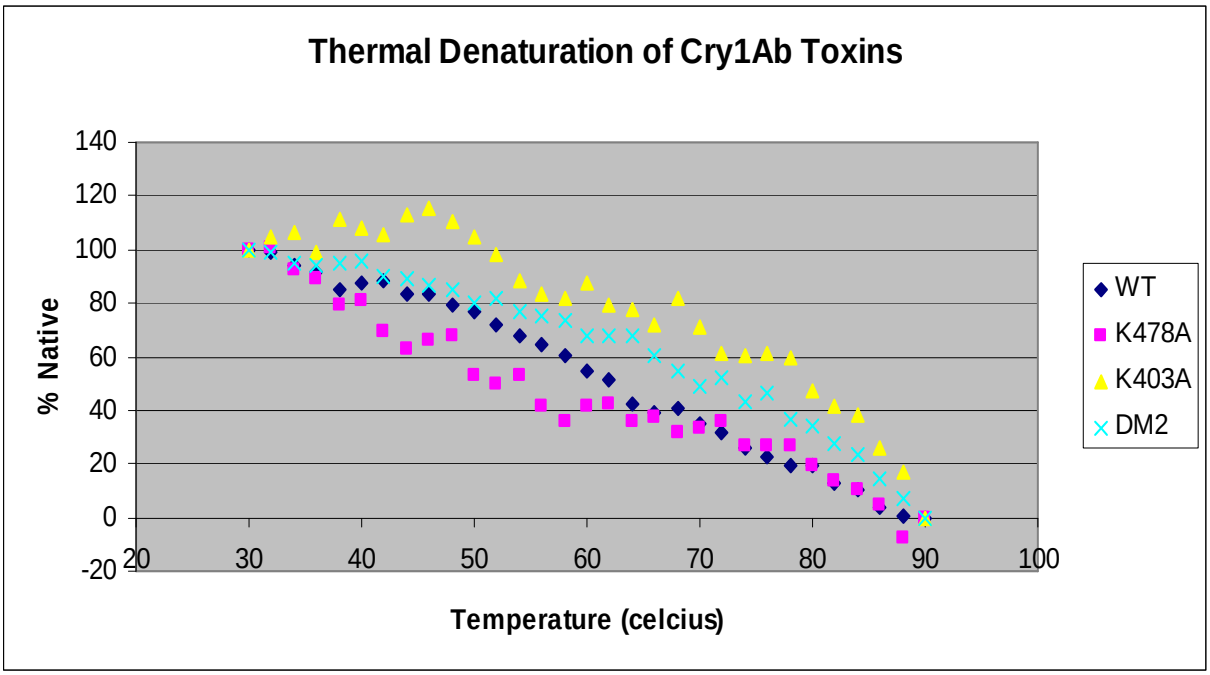

Frame B: Lane (1) purified WT toxin (2) purified K478A (3) MW marker (4) purified K403A (5) purified DM2

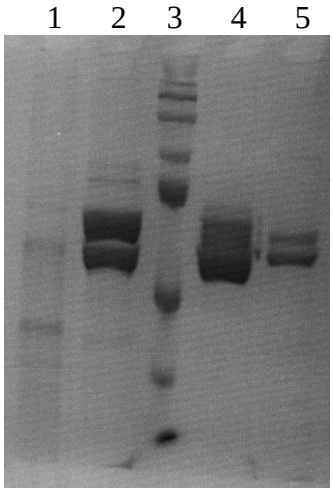

Figure 9: Purified toxin variants

Frame A: lane (1) purified K478A (2) desalted K478A CD sample; resalted (3,4) K490A CD sample and storage sample (5) MW marker (6) desalted K403A CD sample; resalted (7) unconcentrated combination of K403A gel filtration column fractions (8) purified DM1 (9) desalted DM2 CD sample; resalted (10) purified DM2

Frame B: lane (1) concentration of two WT gel filtration column fractions (2) concentration of three WT gel filtration column fractions (3) concentration of Frame A lane 7 (4) MW marker

A

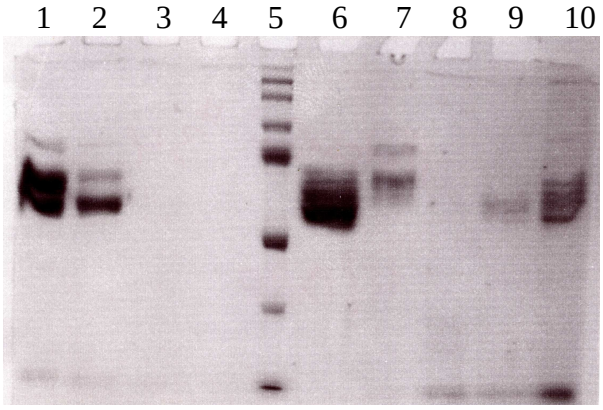

B

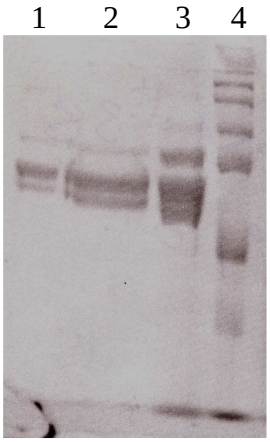

References

1. Pigott, C. R., and Ellar, D. J. (2007) Role of receptors in Bacillus thuringiensis crystal toxin activity, *Microbiol Mol Biol Rev 71*, 255-281.
2. Schnepf, E., Crickmore, N., VanRie, J., Lereclus, D., Baum, J., Feitelson, J., Zeigler, D. R., and Dean, D. H. (1998) *Bacillus thuringiensis* and its pesticidal crystal proteins, *Microbiol. Mol. Biol. Rev. 62*, 775-806.
3. Grochulski, P., Borisova, S., Pusztai-Carey, M., Masson, L., and Cygler, M. (1994) 3-D crystal structure of lepidopteran-specific delta-endotoxin Cry1A(a), in *Proc. VIth Internatl. Coll. Invert. Path. Micro. Control*, Montpellier, France.
4. Aronson, A. I., Geng, C., and Wu, L. (1999) Aggregation of *Bacillus thuringiensis* Cry1A toxins upon binding to target insect larval midgut vesicles., *Appl. Environ. Microbiol. 65*, 2503-2507.
5. Masson, L., Tabashnik, B. E., Liu, Y.-B., Brousseau, R., and Schwartz, J.-L. (1999) Helix 4 of the *Bacillus thuringiensis* Cry1Aa toxin lines the lumen of the ion channel., *J. Biol. Chem. 274*, 31996-32000.

6. Li, J., Carroll, J., and Ellar, D. J. (1991) Crystal structure of insecticidal δ-endotoxin from *Bacillus thuringiensis* at 2.5 Å resolution, *Nature 353*, 815-821.
7. Lee, M. K., Milne, R. E., Ge, A. Z., and Dean, D. H. (1992) Location of a *Bombyx mori* receptor binding region on a *Bacillus thuringiensis* δ-endotoxin, *J. Biol. Chem. 267*, 3115-3121.
8. Burton, S. L., Ellar, D. J., Li, J., and Derbyshire, D. J. (1999) *N*-acetylgalactosamine on the putative insect receptor aminopeptidase N is recognised by a site on the domain III lectin-like fold of a *Bacillus thuringiensis* insecticidal toxin, *J. Mol. Biol. 287*, 1011-1022.
9. Jenkins, J. L., Lee, M. K., Sangadala, S., Adang, M. J., and Dean, D. H. (1999) Binding of *Bacillus thuringiensis* Cry1Ac toxin to *Manduca sexta* aminopeptidase-N receptor is not directly related to toxicity, *FEBS Letts 462*, 373-376.
10. Knowles, B. H. (1994) Mechanism of action of *Bacillus thuringiensis* insecticidal δ-endotoxins, *Adv. Insect Physiol. 24*, 275-308.
11. Nair, M. S., and Dean, D. H. (2008) All domains of Cry1A toxins insert into insect bush border membranes., *J. Biol. Chem. 283*, 26324-28331.
12. Lee, M. K., You, T. H., Curtiss, A., and Dean, D. H. (1996) Involvement of two amino acid residues in the loop region of *Bacillus thuringiensis* Cry1Ab toxin in toxicity and binding to *Lymantria dispar*, *Biochem. Biophys. Res. Commun.* 229, 139–146.
13. Almond, B.D. (1992) Doctoral Dissertation, Genetic Analysis of δ-Endotoxin Cry1A Protein Structure, The Ohio State University.
14. André L. B. Crespo, Terence A. Spencer, Emily Nekl, Marianne Pusztai-Carey, William J. Moar, and Blair D. Siegfried (2008) Comparison and Validation of Methods To Quantify Cry1Ab Toxin from *Bacillus thuringiensis* for Standardization of Insect Bioassays, Appl Environ Microbiol. 74(1): 130–135.
15. Wu, Sheng-Jiun (1996) Doctoral Dissertation, Domain-Function Studies of *Bacillus thuringiensis* Cry3A δ-Endotoxin: A Molecular Genetic Approach, The Ohio State University.
16. Monera, Oscar D., Zhou, Nian E., Kay, Cyril M., Hodges, Robert S. (1993) Comparison of Antiparallel and Parallel Two-stranded α-Helical Coiled-coils, *J. Biol. Chem. 268*, 19218-19227.
17. Alzate, O., You, T., Claybon, M., Osorio, C., Curtiss, A., and Dean, D.H. (2006) Effects of Disulfide Bridges in Domain I of *Bacillus thuringiensis* Cry1Aa ä-Endotoxin on Ion-Channel Formation in Biological Membranes, *Biochemistry 45*, 13597-13605.